Title

MicroRNA-277 targets insulin-like peptides 7 and 8 to control lipid metabolism and reproduction in Aedes aegypti mosquitoes

Journal

Proceedings of the National Academy of Sciences of the United States of America, 114(38)

ISSN

0027-8424

Authors

Ling, Lin
Kokoza, Vladimir A
Zhang, Changyu
et al.

Publication Date

2017-09-19

DOI

10.1073/pnas.1710970114

Peer reviewed

MicroRNA-277 targets *insulin-like peptides 7* and *8* to control lipid metabolism and reproduction in *Aedes aegypti* mosquitoes

Lin Ling[a,b], Vladimir A. Kokoza[a], Changyu Zhang[a], Emre Aksoy[a,c], and Alexander S. Raikhel[a,b,1]

[a]Department of Entomology, University of California, Riverside, CA 92521; [b]Institute of Integrative Genome Biology, University of California, Riverside, CA 92521; and [c]Graduate Program in Genetics, Genomics, and Bioinformatics, University of California, Riverside, CA 92521

Contributed by Alexander S. Raikhel, August 5, 2017 (sent for review June 19, 2017; reviewed by Zach N. Adelman and Michael R. Strand)

Hematophagous female mosquitoes transmit numerous devastating human diseases, including malaria, dengue fever, Zika virus, and others. Because of their obligatory requirement of a vertebrate blood meal for reproduction, these mosquitoes need a lot of energy; therefore, understanding the molecular mechanisms linking metabolism and reproduction is of particular importance. Lipids are the major energy store providing the fuel required for host seeking and reproduction. They are essential components of the fat body, a metabolic tissue that is the insect analog of vertebrate liver and adipose tissue. In this study, we found that microRNA-277 (miR-277) plays an important role in regulating mosquito lipid metabolism. The genetic disruption of miR-277 using the CRISPR-Cas9 system led to failures in both lipid storage and ovary development. miR-277 mimic injection partially rescued these phenotypic manifestations. Examination of subcellular localization of FOXO protein via CRISPR-assisted, single-stranded oligodeoxynucleotide-mediated homology-directed repair revealed that insulin signaling is up-regulated in response to miR-277 depletion. In silico target prediction identified that insulin-like peptides 7 and 8 (*ilp7* and *ilp8*) are putative targets of miR-277; RNA immunoprecipitation and a luciferase reporter assay confirmed that *ilp7* and *ilp8* are direct targets of this miRNA. CRISPR-Cas9 depletion of *ilp7* and *ilp8* led to metabolic and reproductive defects. These depletions identified differential actions of ILP7 and ILP8 in lipid homeostasis and ovarian development. Thus, miR-277 plays a critical role in mosquito lipid metabolism and reproduction by targeting *ilp7* and *ilp8*, and serves as a monitor to control ILP7 and ILP8 mRNA levels.

microRNA | insulin | metabolism | reproduction | mosquito

Blood-feeding mosquitoes are the deadliest animals in the world, transmitting numerous pathogens of dangerous human diseases, causing approximately 1 million human deaths annually worldwide. *Aedes aegypti* transmits arboviruses causing dengue fever, yellow fever, chikungunya, and Zika virus (1–4). An obligatory blood meal is not only the link between human and mosquito hosts in the pathogen's life cycle, but also an evolutionary adaptation of mosquitoes for rapid egg development (5). A single female mosquito has the potential to lay 150 eggs in each gonotrophic cycle. Regarding energy use, reproduction is a costly process, and there is an inevitable trade-off with lipid storage and use because animals mobilize their lipid reserves during reproduction (6–9). Therefore, a thorough understanding of the relationship between lipid metabolism and reproduction at the molecular level is of particular importance for the development of novel and effective approaches to controlling mosquito-borne diseases.

Impaired reproduction is associated with increased lipid stores; for example, removal of ovaries causes fat body hypertrophy and lipid accumulation in a variety of insects (10–13). The fat body, an equivalent of mammalian liver and adipose tissue, is the central depot of nutrients and energy reserve and plays an essential role in intermediary metabolism and reproduction in insects (14, 15). Lipid, the major component of the fat body, is stored as droplets in the cytoplasm (16, 17). During reproduction, lipid reserves are mobilized as the major source of metabolic fuel (18). In *A. aegypti*, blood-triggered reproduction requires an extremely high amount of energy. Indeed, 50% of the lipid store derived from the larval diet persists into adulthood in females (19). In addition, 50% of dietary glucose is converted into lipids and stored in the fat body (19). Regular sugar meals before blood feeding provide female mosquitoes with sufficient lipid stores to carry out gonotrophic cycles (20). For example, during the first cycle, 80% of the lipids found in eggs originate from sugars (21). The molecular pathways linking reproduction and lipid metabolism require further investigation, however.

MicroRNAs (miRNAs), endogenous, small, noncoding RNAs, complex with Argonaute (AGO) proteins and target gene mRNAs to inhibit translation or promote mRNA degradation (22). In animals, the majority of miRNA target sites are found in 3′ UTRs with canonical seed matching. Recently, mounting evidence indicates that some "noncanonical seed" miRNA target sites are highly functional, and that miRNAs can also bind to the coding sequence (CDS) and 5′ UTR of mRNAs (23–26). Consequently, miRNAs have emerged as important gene regulators in a broad range of biological processes in animals and plants via miRNA–mRNA interactions.

In obligatory blood-feeding mosquitoes such as *A. aegypti*, the gonadotrophic cycle is divided into two phases, posteclosion (PE) and post-blood meal (PBM). Female mosquitoes undergo preparation for subsequent blood feeding during the PE phase. A blood meal activates numerous processes and genes in reproductive

Significance

Hematophagous female mosquitoes transmit devastating human diseases. Owing to their obligatory blood feeding, they require an extremely high level of lipid metabolism for reproduction. We found that microRNA-277 (miR-277) plays a critical role in lipid metabolism of *Aedes aegypti* mosquitoes. The genetic disruption of miR-277 using the CRISPR-Cas9 system showed impairment of both lipid storage and ovarian development. Insulin/FOXO signaling was up-regulated after miR-277 depletion. Comprehensive screening and functional identification revealed that insulin-like peptides *ilp7* and *ilp8* are direct targets of miR-277. CRISPR-Cas9 depletions identified differential actions of these ILPs in lipid accumulation and utilization. Thus, miR-277 serves as a monitor that controls ILP7 and ILP8 mRNA levels to maintain the lipid homeostasis required for reproduction.

Author contributions: L.L. and A.S.R. designed research; L.L., V.A.K., C.Z., and E.A. performed research; L.L. contributed new reagents/analytic tools; L.L. and A.S.R. analyzed data; and L.L. and A.S.R. wrote the paper.

Reviewers: Z.N.A., Texas A&M University; and M.R.S., University of Georgia.

The authors declare no conflict of interest.

[1]To whom correspondence should be addressed. Email: alexander.raikhel@ucr.edu.

This article contains supporting information online at www.pnas.org/lookup/suppl/doi:10.1073/pnas.1710970114/-/DCSupplemental.

organs and tissues, leading to rapid egg development during the PBM phase (5, 27). In previous studies, we identified a number of genes implicated in the blood meal-associated signaling cascades essential for blood digestion, yolk protein synthesis, and ovarian development (28–32). In the present study, we demonstrate that miR-277 plays a key role in connecting lipid metabolism and reproduction in female mosquitoes. Abnormal lipid store responses to miR-277 depletion indicate that it participates in regulation of lipid deposition and mobilization. Importantly, we found that miR-277 acts on the insulin-signaling pathway by targeting insulin-like peptides *ilp7* and *ilp8*, affecting energy homeostasis and reproductive function. Thus, miR-277 serves as a monitor to control *ilp7* and *ilp8* transcription levels in the head, maintaining lipid homeostasis and permitting an extremely high metabolism level in the fat body after blood feeding for rapid egg development.

Results

Spatiotemporal Expression Profile of miR-277 in the Female Mosquito. Our previous study of transcriptome-wide miRNA and target gene dynamics showed that miR-277 potentially contributes to metabolic homeostasis (31). Before our functional exploration of miR-277 in the *A. aegypti* mosquito, we determined the distribution of mature miR-277 among different tissues using quantitative real-time PCR (qRT-PCR) analysis. The results show mature miR-277 expression mainly in the heads of mosquitoes (Fig. S1*A*). While in other tissues (fat body, ovary, gut, and Malpighian tubule), its levels were low both before and after a blood meal. We then investigated the time course expression of mature miR-277 in heads from the larval stage until 72 h PBM, when the first batch of eggs is formed. The abundance of mature miR-277 in heads was low during the larval stage, but increased significantly in pupae, reaching its peak by 72 h PE; it then decreased by 1.6-fold at 24 h PBM and maintained this level thereafter (Fig. S1*B*). These results suggest that the high expression of miR-277 in the head may play an important role in tuning the expression of head-specific genes.

Mutation of miR-277 by CRISPR-Cas9 Causes Severe Defects in Primary Follicle Formation and Lipid Accumulation. To further investigate the role of miR-277 in mosquitoes, we generated miRNA-specific mutations using the CRISPR-Cas9 system, a highly efficient genome-editing method. This method can achieve accurate recognition and cleavage through the Cas9 endonuclease, activated directly by base-pairing a synthetic single guide RNA (sgRNA) to the target genomic region. We designed an miR-277–specific sgRNA to develop an miRNA-targeted genomic mutation in *A. aegypti*. At first, the miR-277–specific sgRNA was designed by scanning the miR-277 mature region for the protospacer adjacent motif (PAM) of NGG (the recognition site for *Streptococcus pyogenes* Cas9), where N represents any nucleotide, and 20 bases of complementarity was required for targeting accuracy, excluding the PAM (Fig. S1*C*). We next investigated potential off-target effects of sgRNA using several publicly available bioinformatics tools and found no off-target sites, demonstrating a high specificity of this sgRNA. A guanine was then added to the 5′ end of the 20-bp base-pairing sequence to facilitate transcription by T7 RNA polymerase.

Embryos were injected with a mixture of sgRNA (40 ng/μL) and recombinant Cas9 protein (333 ng/μL). The ratio has been optimized for compromise between high mutagenesis and high survival rates in *A. aegypti* (33). Approximately 41% of injected embryos survived to adulthood and were screened for phenotypic manifestations. First, the mosquitoes survived from larvae to adulthood with normal timing of metamorphosis, lifespan, and sex ratio (females:males, 60:63). Second, Sanger sequencing revealed highly polymorphic mutations at the mature sequence and flanking regions of the miR-277 locus, demonstrating successful genomic destruction by CRISPR-Cas9 (Fig. 1*A*). We dissected the miR-277 mutant mosquitoes to evaluate the ovarian development at 72 h PE and 24 h PBM, and found that 60% of these females displayed inhibited ovarian development. Examination of ovaries at 72 h PE revealed very small primary follicles that completely disappeared, and ovaries melanized by 24 h PBM (Fig. 1*B* and Fig. S2). In a previous study, we found that ovarian development was not affected by use of CRISPR-Cas9 for kynurenine 3-monooxygenase (32); thus, the observed phenotypes likely originated from genetic depletion of miR-277.

To evaluate the effect of miR-277 in regulating metabolism, we stained the lipid droplets in fat body cells with Nile red and found them to be dramatically smaller than those in the wild-type (WT) controls at 72 h PE and 24 h PBM (Fig. 1*C* and Fig. S3). In addition, there was a highly significant difference in triacylglyceride (TAG) levels in WT control and miR-277 mutant mosquitoes at 24 h PBM, with enhanced lipid depletion in the latter (Fig. 2*A*). On the other hand, accumulation of sugar reserves in the form of glycogen was nearly normal (Fig. 2*B*). The miR-277 mutants generated by CRISPR-Cas9 highlight a crucial role of this miRNA in ovarian development and lipid homeostasis.

To verify whether miR-277 depletion is the authentic trigger of the defects in ovarian development and lipid storage, we conducted phenotypic rescue experiments using miR-277 mimic in sgRNA-injected female mosquitoes. Results showed recovery of ovaries (with follicles capable of accumulating considerable amounts of yolk proteins) and increased lipid stores in the fat body cells relative to that seen in the miR-277 group depleted with CRISPR-Cas9 (*ΔmiR277*) (Fig. 3). The adverse phenotypes caused by genomic disruption of miR-277 were alleviated after miR-277 mimic injection, strongly supporting a critical role of miR-277 in the development of ovarian primary follicles and lipid homeostasis in the fat body.

Increasing Nuclear Export of FOXO in Response to miR-277 Depletion. The insulin/FOXO signal transduction pathway is known to affect lipid storage (34). A conserved mechanism during FOXO signaling is downstream activation of the PI3K–Akt axis, which results in phosphorylation of FOXO after insulin treatment, leading to cytoplasmic retention and inhibition of its nuclear transcriptional activity (35, 36). To identify a potential link between the FOXO molecular pathway and the lipid storage defect created by miR-277 deletion, we determined subcellular localization of FOXO protein in fat body cells by means of CRISPR-assisted, single-stranded oligodeoxynucleotide (ssODN)-mediated homology-directed repair (HDR). We designed specific sgRNAs targeting the vicinity of the stop codon of the *FOXO* gene (Fig. 4*A*). We also designed corresponding ssODNs (199 bases; Table S1) to integrate the human influenza hemagglutinin (HA) tag sequence into the genome just upstream of the *FOXO* stop codon (Fig. 4*A*). These constructs (300 ng/μL Cas9 protein, 40 ng/μL miR277-sgRNA, 40 ng/μL FOXO-sgRNA, and 125 ng/μL ssODNs) were introduced into mosquito embryos (n = 2,000) by microinjection. Approximately 9.5% of individuals (n = 190; females, n = 96) survived to adulthood.

We performed immunostaining of fat bodies (dissected from the mutants with undeveloped ovaries at 24 h PBM; n = 59) using anti-HA antibody. In the stained fat bodies, 28.8% (n = 17) of cells were positive with observed HA signals, suggesting successful induction of HDR. In fat bodies of experimental animals, immunofluorescence signal was localized in the cytoplasm and excluded from the nucleus, unlike in the control group (injected with a mixture of 300 ng/μL Cas9 protein, 40 ng/μL FOXO-sgRNA, and 125 ng/μL ssODNs), indicating that miR-277 depletion increases the nuclear export of FOXO protein in fat body cells (Fig. 4*B*). We also performed DNA sequencing of the PCR amplicons of the targeted locus, and found that the HA tag

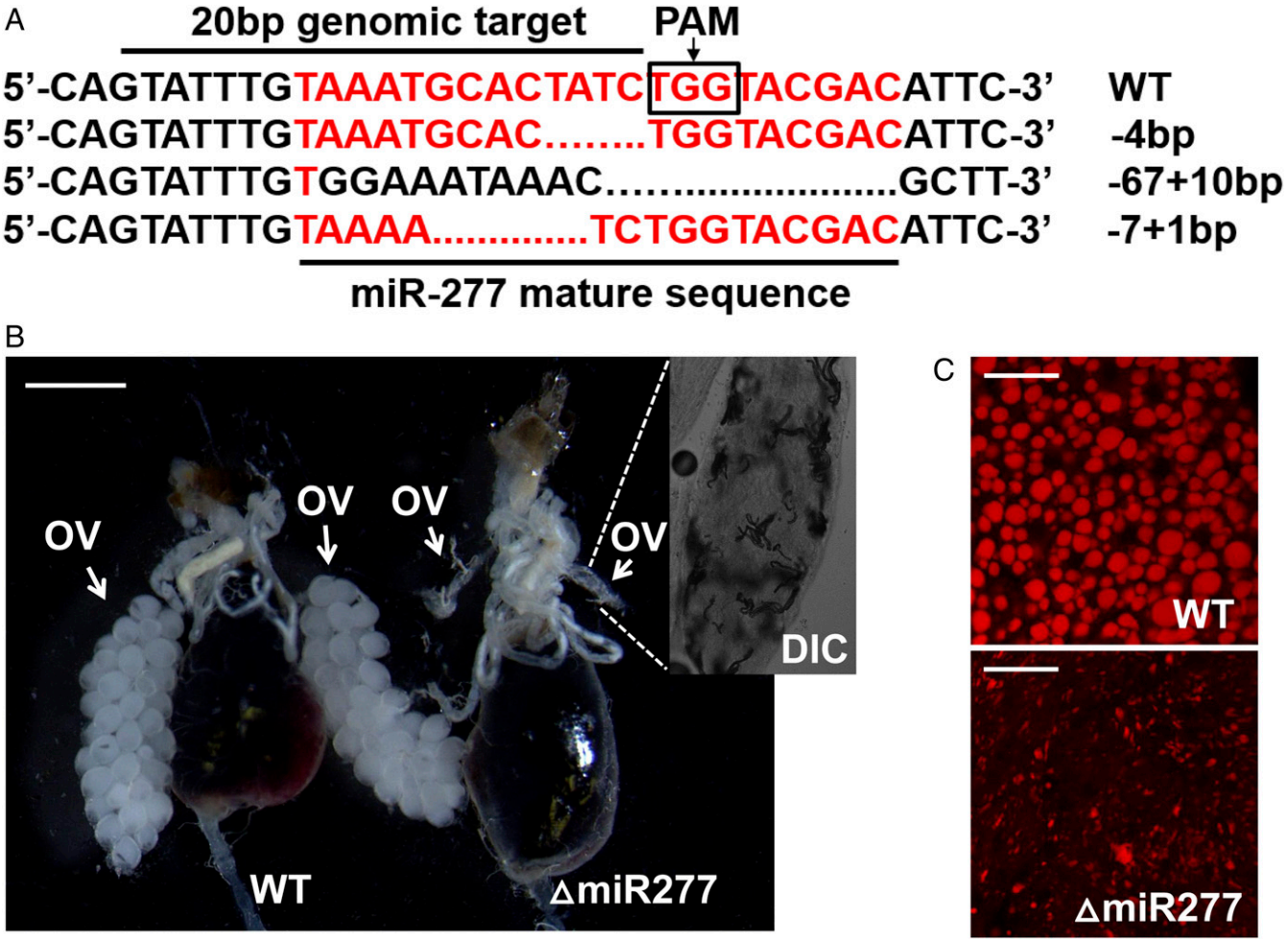

Fig. 1. Genomic disruption of miR-277 by CRISPR-Cas9 blocks ovarian development and reduces the accumulation of lipids in mosquitoes. (*A*) Sequence alignment of sgRNA-targeted genomic region. (*B*) Ovaries were dissected from WT and miR-277 mutant (*ΔmiR277*) female mosquitoes at 24 h PBM. (Scale bar: 1 mm.) The abnormal ovary is magnified using a confocal microscope (Leica SP5) in differential interference contrast (DIC) imaging. OV, ovary. (*C*) Lipid droplets in the fat body dissected from WT females and *ΔmiR277* mutant females (with undeveloped ovaries) at 24 h PBM were detected by Nile red staining and imaged with a Leica SP5 confocal microscope. (Scale bar: 25 μm.)

sequence was integrated, as expected (Fig. 4*C*). Taken together, these results suggest that miR-277 plays a role in controlling the activity of FOXO signaling for reproduction and lipid metabolism in the female mosquito fat body.

***ilp7* and *ilp8* Are the Direct Targets of miR-277.** ILPs are key regulators of metabolism and reproduction (37, 38). Using qRT-PCR, we found that at 24 h PBM, *ilp7* and *ilp8* transcripts were significantly enriched in the heads of *ΔmiR277* female mosquitoes compared with WT controls (Fig. 5*A*). In contrast, other *ilp* genes were not affected (Fig. S4). To verify whether *ilp7* and *ilp8* are the direct targets of miR-277 in female mosquito heads, we performed an RNA immunoprecipitation (RIP) assay with the antibody against *A. aegypti* AGO 1 (anti-AGO), the key component of the RNA-induced silencing complex that mediates miRNA-induced mRNA degradation. The results showed that both ILP7 and ILP8 mRNAs were significantly enriched in the anti-AGO–immunoprecipitated RNAs from heads of mimic miR-277–injected female mosquitoes relative to the control samples (Fig. 5*B*). Furthermore, using in silico tools (PITA, RNAhybrid, microTar, and miRanda), we found that miR-277 had binding sites only in the CDSs of *ilp7* and *ilp8* (Fig. 5*C*). We assessed the binding sites for its response to miR-277 in vitro. The sites were cloned separately downstream of the *Renilla* translational stop codon of the psiCheck-2 vector. When transfected into *Drosophila* Schneider 2 (S2) cells along with the miR-277 mimic, the *ilp7* and *ilp8* reporters yielded 59.18% and 62.97% luciferase activity, respectively, compared with control samples (Fig. 5*D*). Taken together, these data strongly suggest that *ilp7* and *ilp8* are miR-277 direct targets.

To investigate the roles of ILP7 and ILP8 in ovarian development and lipid storage, we used the CRISPR-Cas9 system to disrupt *ilp7* and *ilp8*. We first designed the sgRNAs and introduced them into embryos (n = 500) with Cas9 protein (Fig. 6*A*). Approximately 36% of embryos injected with *ilp7*-sgRNA and 40% of those with *ilp8*-sgRNA survived to adulthood. Our DNA sequencing results showed the successful genomic deletion of target genes (Fig. 6*A*). To analyze the possible impact on ovarian development, we dissected ovaries from the mutants at 72 h PE and 24 h PBM, and found that almost one-half (40 of 86) of *Δilp7* females showed defects, with partially developed ovaries having small but recognizable primary follicles, while 48 of 95 *Δilp8* females had more severe inhibition of primary follicle formation (Fig. S2). Following blood feeding, primary follicles of *Δilp7* females deposited yolk proteins, in contrast to those of *Δilp8* females, which melanized (Fig. 6*B*). We also performed lipid droplet Nile red staining of mutant and WT female mosquitoes and examined them at 72 h PE and 24 h PBM, and also

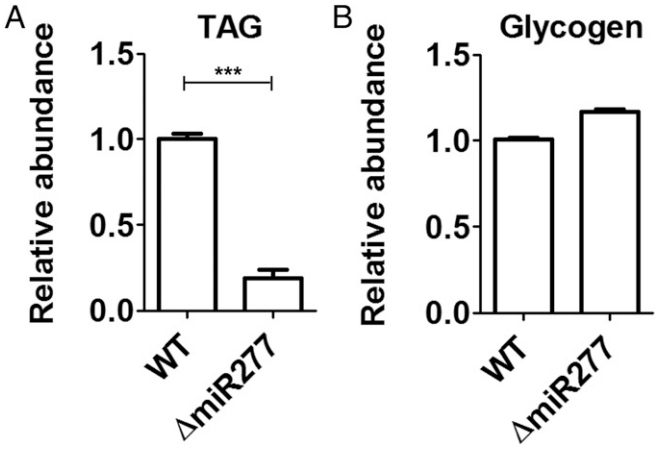

Fig. 2. TAG and glycogen levels in WT and miR-277–depleted mutant females. (*A*) TAG levels in whole mosquitoes. (*B*) Glycogen levels in fat bodies. Fat bodies were dissected from WT and *ΔmiR277* females at 24 h PBM. Data represent three biological replicates with three technical replicates and are shown as mean ± SEM. ***$P < 0.001$.

measured TAG levels. Lipid stores in the fat bodies were dramatically increased in *Δilp7* mutants, but decreased in *Δilp8* mutants, compared with WT controls (Figs. 6*C* and 7*A* and Fig. S3). Interestingly, glycogen levels exhibited the opposite trend, being depleted in the fat body of *Δilp7* mutants and highly elevated in that of *Δilp8* mutants compared with WT controls (Fig. 7*B*).

We then performed qRT-PCR to monitor transcript levels of *ilp7* and *ilp8* in female mosquitoes, and found that both *ilp7* and *ilp8* transcripts were specifically expressed in mosquito heads (Fig. S5*A*). In the head, the abundance of *ilp7* was elevated after the larval stage and peaked at 72 h PE, declining after blood feeding, whereas *ilp8* was increased after the pupal stage and peaked after blood feeding (Fig. S5*B*).

Discussion

Lipid is the major form of energy storage in animals, and the metabolism of lipids provides most of the large amount of energy required during reproduction (18). In *Culex quinquefasciatus*, ∼90% of the energy used by embryogenesis originates from lipids (39). In *A. aegypti*, ∼80% of lipids found in eggs are derived from regular sugar meals before blood feeding (21). In this study, we have demonstrated that miR-277 regulates lipid metabolism by fine-tuning the expression of *ilp7* and *ilp8*, thereby controlling the energy shift required in initiation of ovarian development during gonotrophic cycles. Our previous study showed that in female *A. aegypti* mosquitoes, lipid stores increased dramatically at 72 h PE to shift lipid homeostasis toward the storage of energy reserves for subsequent reproduction (40). In *Drosophila* (41) and *Caenorhabditis elegans* (42), insulin/FOXO signaling regulates the transcription of genes involved in lipid catabolism and anabolism. Using the CRISPR-Cas9 system, we generated the miR-277–depletion mutations in *A. aegypti* mosquitoes and observed severe defects linked to lipid storage and ovarian follicle formation in females. More than one-half of the G_0 females were dramatically arrested at the early stages of primary follicle development and lipid droplet growth, suggesting that miR-277 promotes these functions. Moreover, primary follicles undergo complete resorption and melanization at 24 h PBM. However, the miR-277 mimic injection was able to rescue these phenotypic manifestations, indicating the specific effect of miR-277 mutation on lipid storage and primary follicle development. Although the primary follicles were significantly underdeveloped in the CRISPR-Cas9 miR-277 mutants, they developed nearly normally in the presence of miR-277 mimic. Thus, follicle melanization at 24 h PBM in these mutants could be caused, at least in part, by severe depletion of lipids. Melanization and resorption of primary follicles as a result of nutritional deprivation are well documented in mosquitoes and other insects (43).

The insulin/FOXO signaling pathway plays an essential role in regulating lipid metabolism and reproduction in animals. In *C. elegans*, FOXO activates lipid metabolism enzymes in response to germ line ablation (42, 44, 45). In *Drosophila*, loss of ILP-producing cells or mutation in the insulin receptor gene results in a significant increase in lipid stores (41, 46, 47). Female mice lacking insulin receptor substrate 2 have ovaries with a reduced number of follicles, increased food intake, and obesity (48). In the insulin/FOXO signaling pathway, Akt-mediated phosphorylation of FOXO results in its cytoplasmic retention and inhibition of its transcriptional activity (35, 36). Thus, the subcellular location of FOXO protein can serve as an indicator of signaling activity leading to lipid accumulation. To verify this hypothesis, we used the recently reported HDR-mediated genome editing method, which allows the introduction of targeted insertion of a sequence encoding an epitope or a fluorescent protein that can provide precise mapping of endogenous proteins with subcellular resolution to understand cellular processes (49). We have used this approach to evaluate the response of the insulin/FOXO signaling pathway to miR-277-depletion. We observed cytoplasmic retention of FOXO and a dramatic reduction in lipid droplets, suggesting that miR-277 suppresses the activity of insulin signaling in *A. aegypti* mosquitoes, resulting in lipid mobilization.

Insect ILPs are functional analogs of vertebrate insulin that regulate metabolism and reproduction. Eight ILPs have been described in *A. aegypti* (50). Information on functional role is available only for mosquito ILP3, which has been implicated in activation of the late trypsin gene in the midgut and ecdysteroid production in the ovary (51). In this study, we have described the roles of ILPs 7 and 8 in lipid metabolism and egg development using the genetic approach. Owing to its close proximity, *ilp8* is cotranscribed with *ilp1* and *ilp3* to form polycistronic pre-mRNAs controlled by a single promoter, all of which have independent putative poly-A sites and are capped to generate monocistronic mature mRNAs (50). We found miR-277–binding sites in the CDS of *ilp7* and *ilp8* via in silico prediction. Both *ilp7* and *ilp8* are expressed in the head of larval, pupal, and adult mosquitoes. The depletion of miR-277 increased mRNA levels of *ilp8* without affecting *ilp1* and *ilp3* transcript levels, suggesting that miR-277 targets CDS to flexibly tune the first member (*ilp8*) of the ILP8-ILP1-ILP3 operon. Subsequent experiments further confirmed that *ilp7* and *ilp8* are the direct targets of miR-277 in vivo, based on their increased expression in heads of miR-277 depletion mutants, enrichment of the miR-277-ILP7 and miR-277-ILP8 binding complexes by AGO immunoprecipitation, and degradation of binding site-fused reporters by miR-277 mimic in cell lines. In addition, abnormal lipid storage and ovarian development were observed with the depletion of *ilp7* or *ilp8* mutants. The dramatically increased lipid store in the fat body of *Δilp7* mutants suggests that ILP7 modulates lipid deposition before a blood meal for egg development. Likewise, the decreased lipid store in *Δilp8* mutants suggests that ILP8 modulates lipid mobilization. Moreover, we observed that glycogen levels exhibited the opposite trends in these mosquitoes, which could indicate that ILP7 and ILP8 are also involved in regulation of sugar conversion to lipids.

CRISPR-Cas9 mutations of *ilp7* and *ilp8* affected ovarian development; however, the affects were clearly different. At 72 h PE, in *Δilp7* mutant ovaries and their follicles were half the size of those in WT at 72 h PE; however, follicles of these mosquitoes reached nearly normal size (compared with WT) at 24 h PBM. These mosquitoes had elevated lipid stores, and their

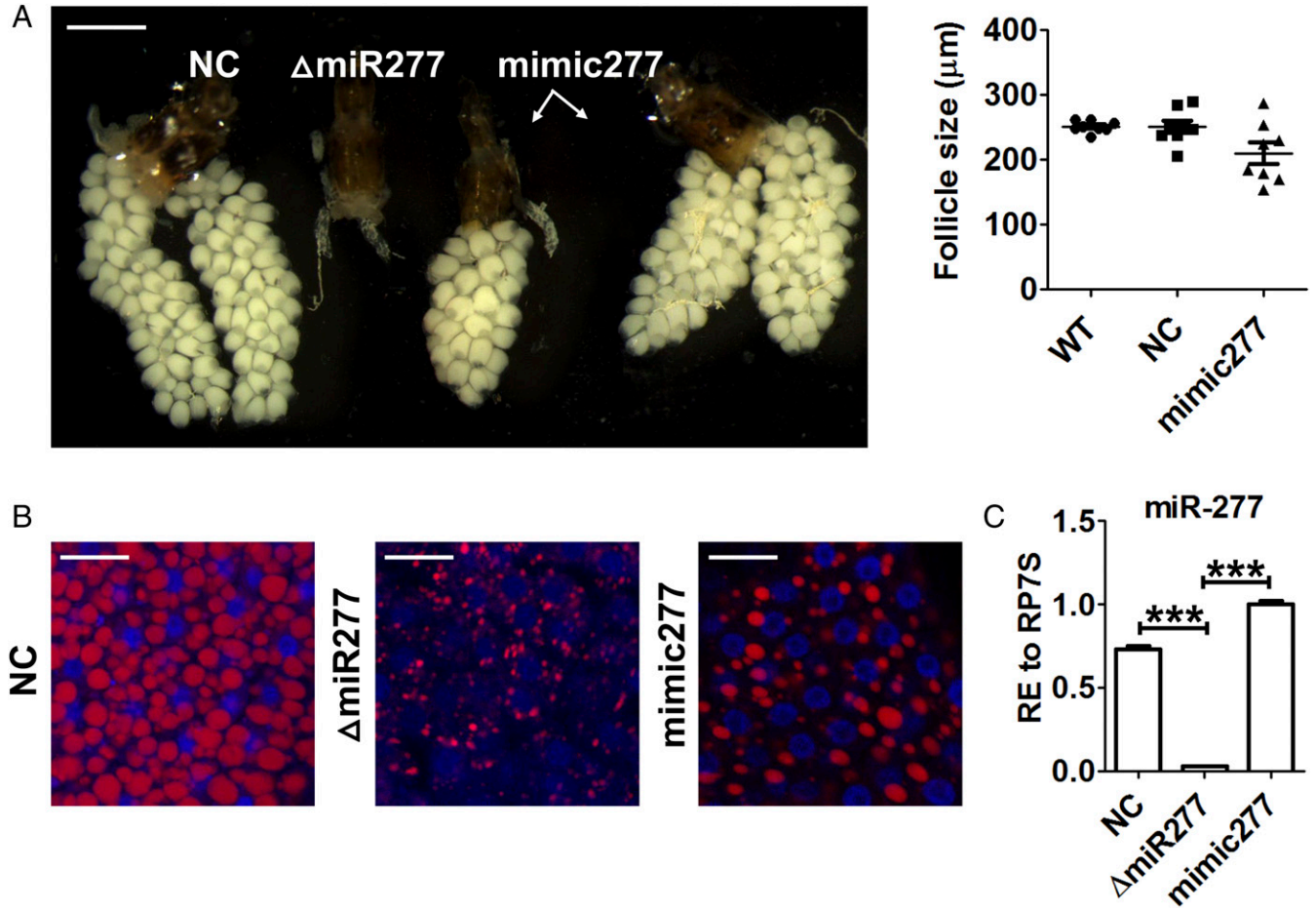

Fig. 3. Mimic miR-277 injection rescues the miR-277 depletion phenotype. (*A*) Ovaries were dissected from negative control (NC), miR-277 mutant (*ΔmiR277*), and mimic miR277-injected female mosquitoes at 24 h PBM. (Scale bar: 1 mm.) (*B*) Lipid droplets in the fat body dissected from NC, *ΔmiR277*, and mimic miR277-injected females at 24 h PBM were detected using Nile Red staining and imaged under a Leica SP5. (Scale bar: 25 μm.) (*C*) Relative expression of mature miR-277 in heads dissected from NC, *ΔmiR277*, and mimic miR277-injected females at 24 h PBM. Data represent three biological replicates with three technical replicates and are shown as mean ± SEM. ***$P < 0.001$.

nutritional status could positively affect oocyte development and yolk accumulation by follicles. In contrast, small *Δilp8* mutant ovaries melanized by 24 h PBM, likely due in part to the severe deprivation of lipids resulting from the lack of sugar conversion in these mosquitoes.

In conclusion, our study has uncovered the essential role of miR-277 in lipid metabolism and ovarian development in *A. aegypti* using the CRISPR-Cas9 system and mimic rescue experiments. Depletion of miR-277 elevated the activity of insulin/FOXO signaling, which is an evolutionarily conserved pathway regulating reproduction and metabolism. We have identified *ilp7* and *ilp8* as direct targets of miR-277, and functional evidence demonstrated that modulation of *ilp7* and *ilp8* by miR-277 is required for lipid metabolism and ovarian development in mosquitoes. Moreover, this study has revealed differential roles of ILP7 and ILP8 in these essential processes.

Materials and Methods

Mosquito Rearing. Adult *A. aegypti* mosquitoes were reared at 27 °C and 80% humidity in cages with access to 10% (wt/vol) sucrose solution and water, and larvae were reared at 27 °C in water with complete larval food, as described previously (29, 52). Blood feeding of adult mosquitoes was performed using White Leghorn chickens. The use of vertebrate animals was approved by the University of California Riverside's Institutional Animal Care and Use Committee.

RNA Extraction and qRT-PCR. Total RNA was extracted from tissues using TRIzol (Invitrogen) according to the manufacturer's instructions and treated with DNase I (Invitrogen). cDNAs for miRNAs were produced from 1 μg of total RNA using the miScript II RT Kit (Qiagen), with HiFlex buffer used for parallel quantities of miRNA and mRNA. qRT-PCR for mature miRNA was performed using the miScript SYBR Green PCR Kit (Qiagen) according to the manufacturer's instructions. qRT-PCR for mRNA quantification was performed using the QuantiFast SYBR Green PCR Kit (Qiagen). Each sample was measured in triplicate, and relative expression was calculated as $2^{-\Delta\Delta Ct}$ and normalized with the housekeeping gene *RPS7*.

Embryonic Injection. sgRNAs were designed as N_{20}(NGG) rule and synthesized using the MEGAscript T7 Transcription Kit (Ambion). sgRNAs were purified using the MEGAclear Transcription Clean-Up Kit (Ambion) following the manufacturer's protocol. Cas9 protein with NLS (PNA Bio) was purchased injection-ready and stored as 1 mg/mL reconstitutions. ssODN donors for HDR were designed and synthesized as Ultramer oligos (Integrated DNA Technologies) containing the 27-base HA tag sequence, flanked by homologous arms of 86 bases. Microinjection into preblastoderm embryos was performed with a mixture of sgRNAs (40 ng/μL) and Cas9 protein (333 ng/μL). For HDR, the microinjection components were ssODN donors (125 ng/μL), sgRNAs (40 ng/μL each), and Cas9 protein (300 ng/μL). The ratio was optimized according to previously described protocols (33). The embryos were injected into the posterior pole at an angle of 10–25°, hatched at 5 d after injection, and were then reared to adulthood according to described protocols (53). Females were crossed and blood fed for phenotypic analysis.

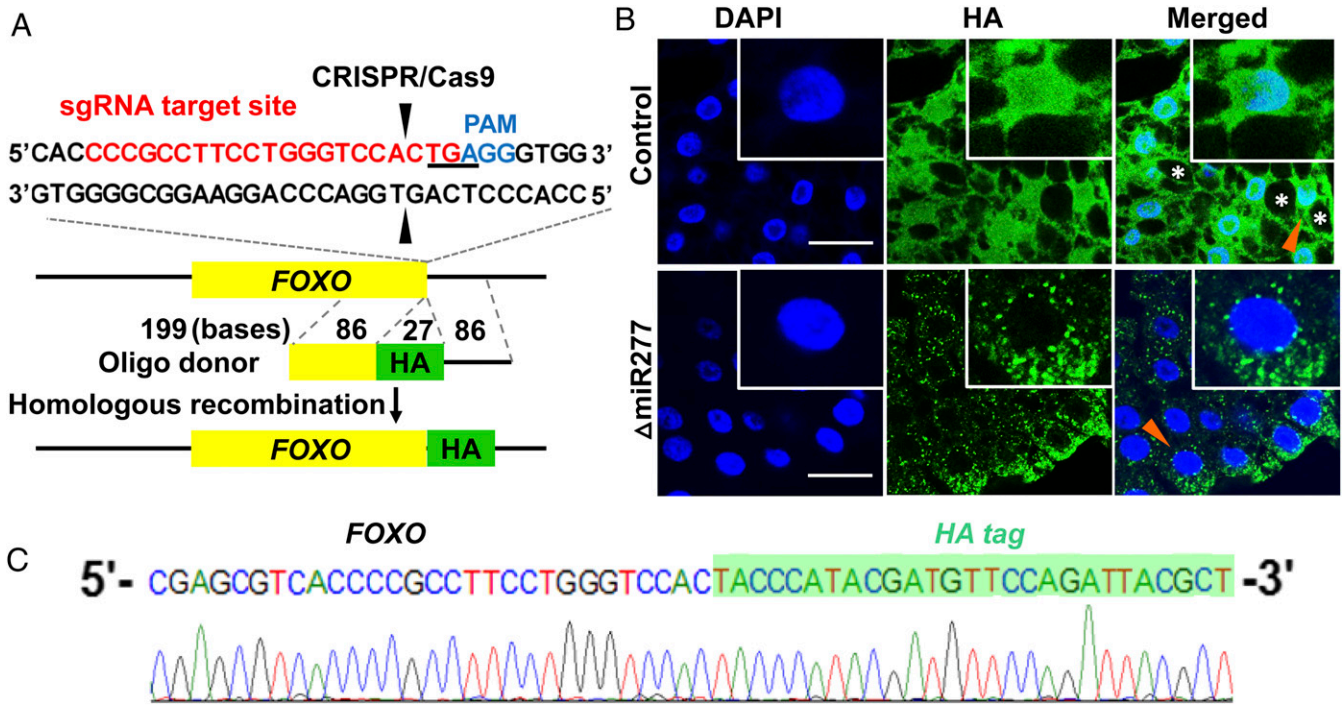

Fig. 4. In vivo single-cell labeling of endogenous FOXO protein by HDR. (*A*) Graphical representation of the mosquito genomic loci of *FOXO* showing the target site for Cas9, sgRNA, and ssODN. The sequence of the sgRNA target site is labeled in red. The PAM sequence is labeled in blue. The stop codon of *FOXO* is underscored. The Cas9 cleavage site is indicated by a black arrowhead. (*B*) Confocal microscopy images of the fat body dissected from control females and *ΔmiR277* mutant females at 24 h PBM showing the DAPI signal (blue) and the HA tag (green) fused to the C terminus of endogenous *FOXO*. (Scale bar: 25 μm.) (*Insets*) Magnified views of single cells indicated in the tissue by arrowheads. Asterisks denote lipid droplets in control tissue. (*C*) DNA sequencing analysis of the PCR products for *FOXO-HA*. The HA tag sequence is in green.

Mimic Treatment. Mimic and AllStars Negative Control siRNA were purchased from Qiagen. At 24 h PE, 100 pmol mimic or 100 pmol negative control siRNA was microinjected into the thoraces of female mosquitoes. Mosquitoes were allowed to recover for 3–4 d before blood feeding, and were dissected at 24 h after a blood meal.

Histology. Tissues were fixed in 4% (vol/vol) paraformaldehyde and rinsed with PBS-T [0.3% (vol/vol) Triton X-100 in PBS]. For immunohistochemistry, samples were kept in 3% (wt/vol) BSA in PBS-T for 1 h and then incubated overnight with primary antibody mouse anti-HA (1:1,000; Abcam). After a 2-h incubation with Alex Fluor Plus 488-conjugated secondary antibody (goat anti-mouse; Invitrogen), followed by DAPI staining (ProLong Diamond Antifade Mountant with DAPI; Invitrogen), the samples were examined with a Leica SP5 confocal laser scanning microscope. For lipid droplet staining, fat bodies were incubated in Nile red solution (20% glycerol in PBS, with a 1:10,000 dilution of 10% Nile red in DMSO) and examined with a Leica SP5 confocal laser-scanning microscope.

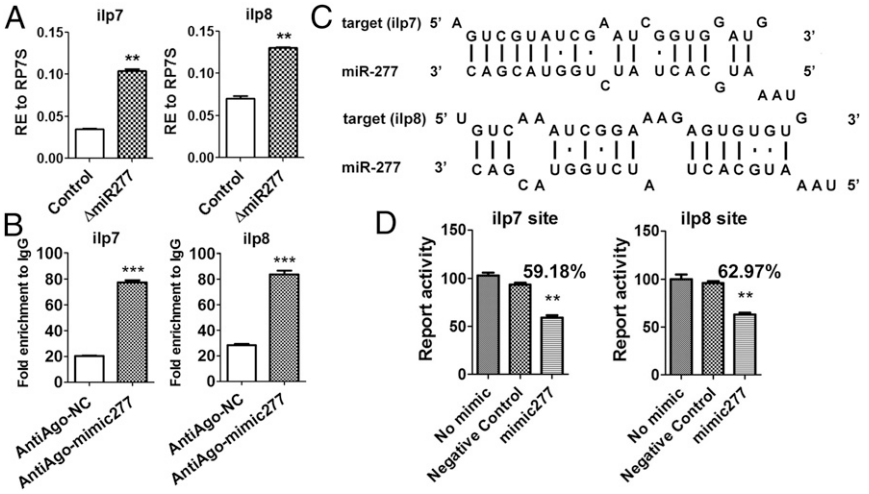

Fig. 5. The genes encoding the ILP7 and ILP8 are the direct targets of miR-277. (*A*) The expression levels of *ilp7* and *ilp8* were increased significantly in the heads of ρmiR277 mutant females compared with control (WT). (*B*) RIP assay demonstrating that miR-277 directly targets *ilp7* and *ilp8* in vivo. The mRNAs of *ilp7* and *ilp8* were significantly enriched after immunoprecipitation with antibody against AGO-1. Data represent the fold enrichment to the IgG-precipitated mRNA. (*C*) The putative miR-277 binding sites in *ilp7* and *ilp8* were predicted using software. (*D*) Luciferase reporter assay showing that miR-277 directly degrades the targets in vitro. Data represent three biological replicates with three technical replicates and are shown as mean ± SEM. $^{**}P < 0.01$; $^{***}P < 0.001$.

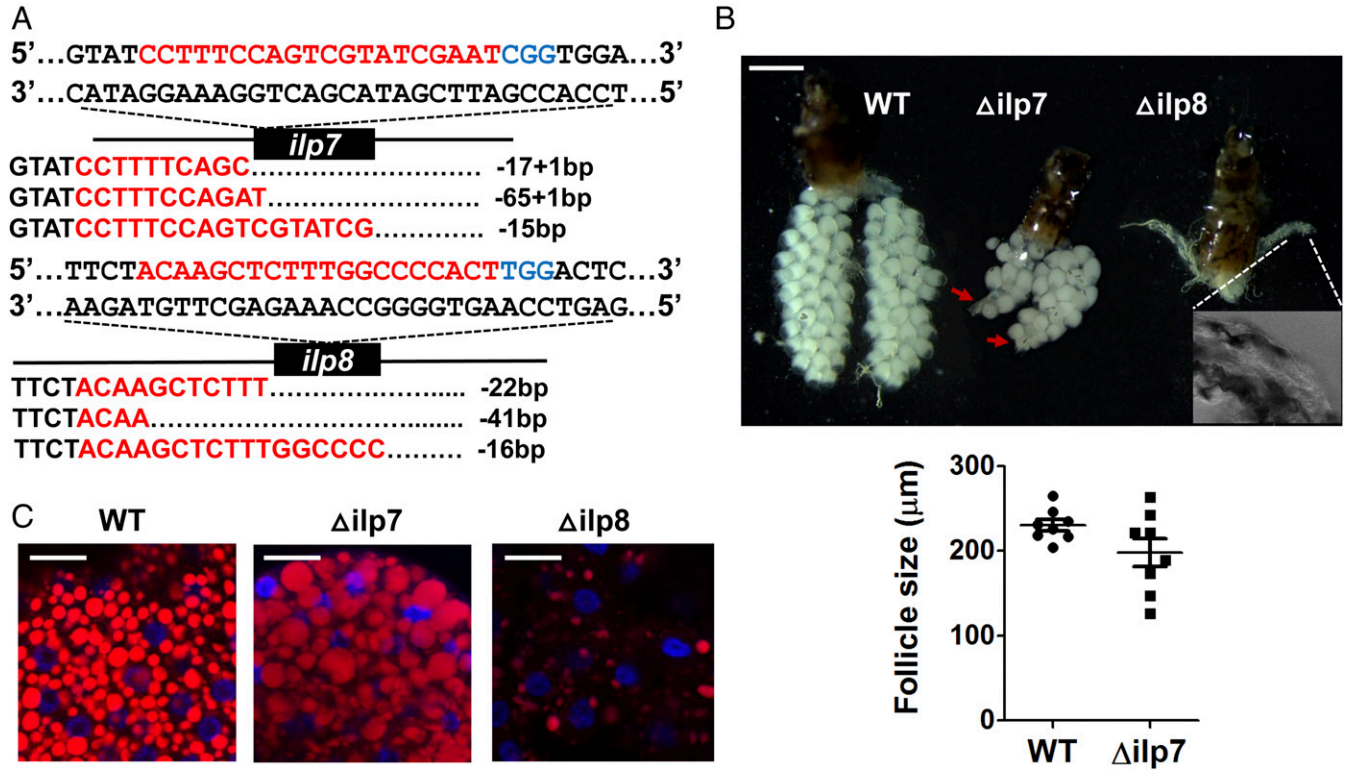

Fig. 6. Genomic disruption of *ilp7* or *ilp8* by CRISPR-Cas9 results in abnormal phenotypes of ovarian development and lipid storage in mosquitoes. (*A*) Graphical representation of the target sites for Cas9 and sgRNAs (red) with the PAM in blue. Sequence alignments of sgRNA-targeted genomic region are listed below. (*B*) Ovaries were dissected from WT, *Δilp7*, and *Δilp8* female mosquitoes at 24 h PBM. (Scale bar: 1 mm.) The ovarian ends with no follicles are indicated by the red arrows. The melanized abnormal ovary is magnified with a Leica SP5 confocal microscope in DIC imaging. (*C*) Lipid droplets in the fat body dissected from WT females and *Δilp7*/*Δilp8* mutant females (with abnormal ovaries) at 24 h PBM were detected using Nile red staining and examined with a Leica SP5 confocal midcroscope. (Scale bar: 25 μm.)

Determination of TAG Levels. TAG levels were measured using the Triglyceride Colorimetric Assay (Cayman) following the manufacturer's instructions. In brief, six mosquitoes were homogenized in 100 μL of Diluent Assay Reagent (Cayman). Then 10 μL of supernatant was incubated with Enzyme Mixture Solution (Cayman). The TAG contents from the measurements were normalized to protein levels in the supernatant of the samples determined using a BCA protein assay (Thermo Fisher Scientific).

Determination of Glycogen Levels. Glycogen levels were measured using the Glycogen Assay Kit (Cayman) following the manufacturer's instructions. In brief, six fat bodies were homogenized in 100 μL of Diluent Assay Buffer (Cayman), and 10 μL of supernatant was incubated with Enzyme Solution and Developer Mixture (Cayman). The of glycogen contents from the measurements were normalized to protein levels in the supernatant of the samples determined using a BCA protein assay (Thermo Fisher Scientific).

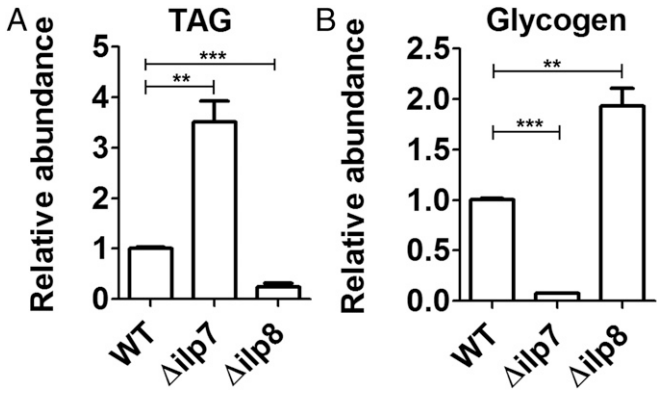

Fig. 7. TAG and glycogen levels in *ilp7*- and *ilp8*-depleted mutant females. (*A*) TAG levels in whole mosquitoes. (*B*) Glycogen levels in fat bodies. Fat bodies were dissected from WT, *Δilp7*, and *Δilp8* females at 24 h PBM. Data represent three biological replicates with three technical replicates and are shown as mean ± SEM. $^{**}P < 0.01$; $^{***}P < 0.001$.

RIP Assay. An EMD Millipore kit was used to perform the RIP assay, following the manufacturer's instructions. In brief, dissected heads were collected in ice-cold lysis buffer (EMD Millipore) and crushed using a tissue homogenizer. Magnetic beads were coated with 5 μg of *A. aegypti* AGO-1 antibody (custom made; GenScript) or normal mouse IgG protein (EMD Millipore). AGO1-bound mRNAs were pulled down from homogenates with AGO1-linked magnetic beads. After digestion with protease K, immunoprecipitated RNAs were released. Finally, the purified RNA samples were used for cDNA synthesis, and target genes were quantified using qRT-PCR.

Computational Prediction and Luciferase Report Assay. Computational target prediction was performed using PITA, microTar, RNAhybrid, and miRanda. The binding sites were inserted into a psiCheck-2 vector (Promega) and located downstream of the *Renilla* stop codon. Then 100 ng of psiCheck-2 and 100 nM synthetic aae-miR-277 miScript miRNA Mimic (Qiagen) or AllStars Negative Control siRNA (Qiagen) were cotransfected into *Drosophila* S2 cells (Invitrogen) using FuGENE HD Transfection Reagent (Promega). Cells were cultured at 28 °C in Schneider's *Drosophila* medium (Gibco) containing 10% (vol/vol) heat-inactivated FBS (Gibco) and 1× antibiotic-antimycotic (Gibco). The luciferase activity assay was performed at 48 h after transfection using the Promega Dual Luciferase Reporter Assay System. Each sample was measured in triplicate, and transfections were repeated three times.

Statistical Analysis. All statistical values are presented as mean ± SEM. Means were compared using Student's *t* test at the following significance levels: $^{*}P < 0.05$, $^{**}P < 0.01$, and $^{***}P < 0.001$. Statistical analyses were performed using GraphPad Prism 6.

ACKNOWLEDGMENTS. This work was supported by National Institutes of Health Grants R01 AI113729 and R01 AI036959 (to A.S.R.).

1. Barrett ADT, Higgs S (2007) Yellow fever: A disease that has yet to be conquered. *Annu Rev Entomol* 52:209–229.
2. McNeil CJ, Shetty AK (2017) Zika virus: A serious global health threat. *J Trop Pediatr* 63:242–248.
3. Tsetsarkin KA, Chen R, Weaver SC (2016) Interspecies transmission and chikungunya virus emergence. *Curr Opin Virol* 16:143–150.
4. Weaver SC, et al. (2016) Zika virus: History, emergence, biology, and prospects for control. *Antiviral Res* 130:69–80.
5. Attardo GM, Hansen IA, Raikhel AS (2005) Nutritional regulation of vitellogenesis in mosquitoes: Implications for anautogeny. *Insect Biochem Mol Biol* 35:661–675.
6. Flatt T (2011) Survival costs of reproduction in *Drosophila*. *Exp Gerontol* 46:369–375.
7. Fontana R, Della Torre S (2016) The deep correlation between energy metabolism and reproduction: A view on the effects of nutrition for women fertility. *Nutrients* 8:87.
8. Shanley DP, Kirkwood TBL (2000) Calorie restriction and aging: A life-history analysis. *Evolution* 54:740–750.
9. Bradley TJ, Simmons FH (1997) An analysis of resource allocation in response to dietary yeast in *Drosophila melanogaster*. *J Insect Physiol* 43:779–788.
10. Judd ET, et al. (2011) Ovariectomy in grasshoppers increases somatic storage, but proportional allocation of ingested nutrients to somatic tissues is unchanged. *Aging Cell* 10:972–979.
11. Socha R, Sula J, Kodrik D, Gelbic I (1991) Hormonal-control of vitellogenin synthesis in *Pyrrhocoris-apterus* (L) (Heteroptera). *J Insect Physiol* 37:805–816.
12. Strong L (1967) Feeding activity sexual maturation hormones and water balance in female African migratory locust. *J Insect Physiol* 13:495–507.
13. Thomsen E, Hamburger K (1955) Oxygen consumption of castrated females of the blow-fly, *Calliphora-erythrocephala* Meig. *J Exp Biol* 32:692–699.
14. Law JH, Wells MA (1989) Insects as biochemical models. *J Biol Chem* 264:16335–16338.
15. Mirth CK, Riddiford LM (2007) Size assessment and growth control: How adult size is determined in insects. *BioEssays* 29:344–355.
16. Arrese EL, Soulages JL (2010) Insect fat body: Energy, metabolism, and regulation. *Annu Rev Entomol* 55:207–225.
17. Olofsson SO, et al. (2009) Lipid droplets as dynamic organelles connecting storage and efflux of lipids. *Biochim Biophys Acta* 1791:448–458.
18. Hansen M, Flatt T, Aguilaniu H (2013) Reproduction, fat metabolism, and life span: What is the connection? *Cell Metab* 17:10–19.
19. Zhou G, Pennington JE, Wells MA (2004) Utilization of pre-existing energy stores of female *Aedes aegypti* mosquitoes during the first gonotrophic cycle. *Insect Biochem Mol Biol* 34:919–925.
20. Briegel H, Hefti M, DiMarco E (2002) Lipid metabolism during sequential gonotrophic cycles in large and small female *Aedes aegypti*. *J Insect Physiol* 48:547–554.
21. Ziegler R, Ibrahim MM (2001) Formation of lipid reserves in fat body and eggs of the yellow fever mosquito, *Aedes aegypti*. *J Insect Physiol* 47:623–627.
22. Ha M, Kim VN (2014) Regulation of microRNA biogenesis. *Nat Rev Mol Cell Biol* 15: 509–524.
23. Helwak A, Kudla G, Dudnakova T, Tollervey D (2013) Mapping the human miRNA interactome by CLASH reveals frequent noncanonical binding. *Cell* 153:654–665.
24. Liu G, Zhang R, Xu J, Wu CI, Lu X (2015) Functional conservation of both CDS- and 3′ UTR-located microRNA binding sites between species. *Mol Biol Evol* 32:623–628.
25. Moretti F, Thermann R, Hentze MW (2010) Mechanism of translational regulation by miR-2 from sites in the 5′ untranslated region or the open reading frame. *RNA* 16: 2493–2502.
26. Xu W, San Lucas A, Wang Z, Liu Y (2014) Identifying microRNA targets in different gene regions. *BMC Bioinformatics* 15(Suppl 7):S4.
27. Raikhel AS, et al. (2002) Molecular biology of mosquito vitellogenesis: From basic studies to genetic engineering of antipathogen immunity. *Insect Biochem Mol Biol* 32:1275–1286.
28. Bryant B, Macdonald W, Raikhel AS (2010) microRNA miR-275 is indispensable for blood digestion and egg development in the mosquito *Aedes aegypti*. *Proc Natl Acad Sci USA* 107:22391–22398.
29. Liu S, Lucas KJ, Roy S, Ha J, Raikhel AS (2014) Mosquito-specific microRNA-1174 targets serine hydroxymethyltransferase to control key functions in the gut. *Proc Natl Acad Sci USA* 111:14460–14465.
30. Lucas KJ, et al. (2015) MicroRNA-8 targets the wingless signaling pathway in the female mosquito fat body to regulate reproductive processes. *Proc Natl Acad Sci USA* 112:1440–1445.
31. Zhang X, Aksoy E, Girke T, Raikhel AS, Karginov FV (2017) Transcriptome-wide microRNA and target dynamics in the fat body during the gonadotrophic cycle of *Aedes aegypti*. *Proc Natl Acad Sci USA* 114:E1895–E1903.
32. Zhang Y, et al. (2016) microRNA-309 targets the homeobox gene SIX4 and controls ovarian development in the mosquito *Aedes aegypti*. *Proc Natl Acad Sci USA* 113: E4828–E4836.
33. Kistler KE, Vosshall LB, Matthews BJ (2015) Genome engineering with CRISPR-Cas9 in the mosquito *Aedes aegypti*. *Cell Rep* 11:51–60.
34. Saltiel AR, Kahn CR (2001) Insulin signalling and the regulation of glucose and lipid metabolism. *Nature* 414:799–806.
35. Ogg S, et al. (1997) The fork head transcription factor DAF-16 transduces insulin-like metabolic and longevity signals in *C. elegans*. *Nature* 389:994–999.
36. Puig O, Marr MT, Ruhf ML, Tjian R (2003) Control of cell number by *Drosophila* FOXO: Downstream and feedback regulation of the insulin receptor pathway. *Genes Dev* 17: 2006–2020.
37. Grönke S, Clarke DF, Broughton S, Andrews TD, Partridge L (2010) Molecular evolution and functional characterization of *Drosophila* insulin-like peptides. *PLoS Genet* 6: e1000857.
38. Wu Q, Brown MR (2006) Signaling and function of insulin-like peptides in insects. *Annu Rev Entomol* 51:1–24.
39. Vanhandel E (1993) Fuel metabolism of the mosquito (*Culex quinquefasciatus*) embryo. *J Insect Physiol* 39:831–833.
40. Wang X, et al. (2017) Hormone and receptor interplay in the regulation of mosquito lipid metabolism. *Proc Natl Acad Sci USA* 114:E2709–E2718.
41. DiAngelo JR, Birnbaum MJ (2009) Regulation of fat cell mass by insulin in *Drosophila melanogaster*. *Mol Cell Biol* 29:6341–6352.
42. McCormick M, Chen K, Ramaswamy P, Kenyon C (2012) New genes that extend *Caenorhabditis elegans*' lifespan in response to reproductive signals. *Aging Cell* 11: 192–202.
43. Clifton ME, Noriega FG (2012) The fate of follicles after a blood meal is dependent on previtellogenic nutrition and juvenile hormone in *Aedes aegypti*. *J Insect Physiol* 58: 1007–1019.
44. Goudeau J, et al. (2011) Fatty acid desaturation links germ cell loss to longevity through NHR-80/HNF4 in *C. elegans*. *PLoS Biol* 9:e1000599.
45. Wang MC, O'Rourke EJ, Ruvkun G (2008) Fat metabolism links germline stem cells and longevity in *C. elegans*. *Science* 322:957–960.
46. Böhni R, et al. (1999) Autonomous control of cell and organ size by CHICO, a *Drosophila* homolog of vertebrate IRS1-4. *Cell* 97:865–875.
47. Broughton SJ, et al. (2005) Longer lifespan, altered metabolism, and stress resistance in *Drosophila* from ablation of cells making insulin-like ligands. *Proc Natl Acad Sci USA* 102:3105–3110.
48. Burks DJ, et al. (2000) IRS-2 pathways integrate female reproduction and energy homeostasis. *Nature* 407:377–382.
49. Mikuni T, Nishiyama J, Sun Y, Kamasawa N, Yasuda R (2016) High-throughput, high-resolution mapping of protein localization in mammalian brain by in vivo genome editing. *Cell* 165:1803–1817.
50. Riehle MA, Fan Y, Cao C, Brown MR (2006) Molecular characterization of insulin-like peptides in the yellow fever mosquito, *Aedes aegypti*: Expression, cellular localization, and phylogeny. *Peptides* 27:2547–2560.
51. Gulia-Nuss M, Robertson AE, Brown MR, Strand MR (2011) Insulin-like peptides and the target of rapamycin pathway coordinately regulate blood digestion and egg maturation in the mosquito *Aedes aegypti*. *PLoS One* 6:e20401.
52. Roy SG, Hansen IA, Raikhel AS (2007) Effect of insulin and 20-hydroxyecdysone in the fat body of the yellow fever mosquito, *Aedes aegypti*. *Insect Biochem Mol Biol* 37: 1317–1326.
53. Kokoza V, et al. (2010) Blocking of *Plasmodium* transmission by cooperative action of cecropin A and defensin A in transgenic *Aedes aegypti* mosquitoes. *Proc Natl Acad Sci USA* 107:8111–8116.